

## Synthesis and Characterization of Some Nano Composites of Derivations Benzimidazole and Study its activity anti bacteria and antifungal

Diana AbdAlkreem Al-Rifai\*, Malath Khalaf Rasheed

Department of Chemistry, College of Education, University of Samarra, Samarra, Iraq

<https://doi.org/10.54153/sjpas.2022.v4i2.361>

### Article Information

Received: 04/02/2022

Accepted: 20/03/2022

### Keywords:

GrapheneOxide, Graphene, Benzimidazole, Nano Composites

### Corresponding Author

E-mail:

[deyana.abd@uosamarra.edu.iq](mailto:deyana.abd@uosamarra.edu.iq)

Mobile: 07702646676

### Abstract

In this study, various nanoparticles were prepared for graphene plates, which were activated by using benzimidazole compounds. Oxidation penetrates between layers within the graphite crystals to remove the layers partially or completely through chemical peeling, the nanoparticle of the graphene was prepared in two steps. The first step was the preparation of the graphene oxide (GO) (Hummer method) through the interaction of active groups. In the caravan structures with oxidation and acid factors for the preparation of the graphene oxide. The second step was synthesis of benzimidazole derivatives from the reaction of the compound 4-methyl ortho phenylline diamine and ortho phenylline diamine with different carboxylic acids in the presence of ammonium chloride as a catalyst, using microwave irradiation method. The thierde step was the reaction of the nano graphene oxide with benzimidazole derivatives. The effect of some nano Composites on the growth of one fungi of the yeast species Candida and the isolates of bacteria from Bacillus Puimilus and Nystatin for fungi and neomycin sulfate for bacteria have been used. and the results indicate that the nano Composites have the ability to inhibit the used fungi and bacteria

### Introduction

Graphene is a promising material due to its unique mechanical, electrical and thermal properties. It is composed of pure carbon linked to a flat hexagonal pattern hybridized SP<sup>2</sup> form two-dimensional structures, and is described as the building block of all graphite materials because of its two dimensional structures, monolayer graphite has a theoretically defined surface area of (2630 m<sup>2</sup>.g<sup>-1</sup>), Which are much larger than black carbon pipes and carbon nanotubes [1].

It is the best conductor of heat, in addition to being completely transparent, and because of its high transparency, it has been used in the manufacture of touch screens and photovoltaic cells [2]. It is also of limited use because of its high cost and also has optical applications, consisting of

a thin two- dimensional layer that can be used in electronic optical devices such as transistors [3].

Benzimidazole is abenzo-fused imidazole which constitutes an important class of heterocyclic compound in numerous natural and synthetic compounds in medicinal chemistry for new drug development [4]. The most prominent benzimidazole compound in nature is N-riboseyl dimethylbenzimidazole, which serves as an axial ligand for cobalt in vitamin B<sup>12</sup> core [5].

## **Material and Methods.**

### **Materials and equipment used**

All the chemicals that applied in our study are obtainable from Fluka. and Sigma Aldrich but the graphite chips (99.9%) were purchased from USH. The Melting points have been specified by Electro thermal capillary apparatus. Completing of the reaction was monitored by thin layer chromatography (TLC) using Merck sili-ca coated plates and as mobile phase a mixture of hexane and ethyl acetate. Infrared spectra were obtained using ATR technique Shimadzu 8400S, Fourier Transforms Infrared spectroscopy SHIMADZU in the range (400-4000) cm<sup>-1</sup>. The <sup>1</sup>H-NMR spectra were obtained on a Bruker, model ultra-shield 400MHz in the laboratories of the University of Science and Technology (Tehran). Using tetra methyl silane (TMS) as internal reference and DMSO-d<sub>6</sub> as solvent. X - ray diffraction device (Shimadzu - XRD-6000), Scanning Electron Microscope Device (TE SCAN)/ Belsorp Mini II/ Czech Republic), and Atomic force microscope device (AFM Icon. Bruker Q600).

### **Synthesis Graphene Oxide (GO)**

In a snow bath, a 600 mL beaker was added and 46 mL of concentrated sulfuric acid (H<sub>2</sub>SO<sub>4</sub>) was added with continuous magnetic stirring. At 0 C° 1.5 g of sodium nitrate was gradually added with stirring, and after 15 minutes the graphite was added 1 g over a period of 10 minutes. Then add to the mixture 6 g potassium permanganate slowly and cautiously gradually within 10 minutes while maintaining the temperature below 10 C° for two hours, and then raise the mixture of the ice bath and then add 46 ml of distilled water drop by drop with stirring for a quarter of an hour with the raise The temperature is 98 C° , then distilled water is added 140 ml warm temperature below 50 C° , Leave to stir for 10 minutes, then add 15 ml of hydrogen peroxide H<sub>2</sub>O<sub>2</sub> concentration of 30% with stirring for 30 minutes, and then divide the mixture into two parts and add each part 150 ml distilled water and left to precipitate for 24 hours pour and wash with (HCl) 10% once Five times with deionized water and until the acidic function (pH = 7) arrived, it was dried at a temperature of 60-70 Co [6]. Figure (1) shows the preparation of Graphene Oxide (GO)

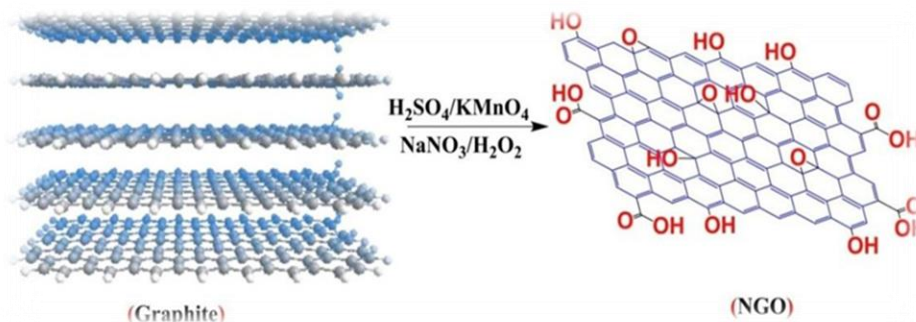


Figure: (1): Illustrates the process of preparing nano Graphene Oxide (GO)

## Synthesis benzimidazole compounds

### Synthesis of benzimidazole derivatives (D<sub>1</sub>, D<sub>3</sub>, D<sub>7</sub>, D<sub>9</sub>, D<sub>10</sub>) [7]

Take of carboxylic acids (0.0046mole) (Ibuprofen, Naproxen, Mefenamic acid, Captopril and Aspirine) was dissolved in (20 ml) of Toluene and added 5drops from Hydrochloric acid with stirring for 10 min. at room temperature, the mixture was added (0.0046mole,0.5g) O-phenylendiamine or 4-methyl-O-phenylendiamine and added NH<sub>4</sub>Cl (0.0046mole). The reaction mixture was refluxed in the microwave for 5-8 minutes (425watt). The completion of reaction was confirmed by TLC (ethylacetate: hexane,1:3 v/v), The reaction mixture was colded and the product was precipitated. The contents were filtered and product was washed with water twice and it was dried and purified by recrystallization from ethanol to give pure product. Figure (2), table (1) Show some physical properties of the synthesized compounds (D<sub>1</sub>, D<sub>3</sub>, D<sub>7</sub>, D<sub>9</sub>, D<sub>10</sub>)

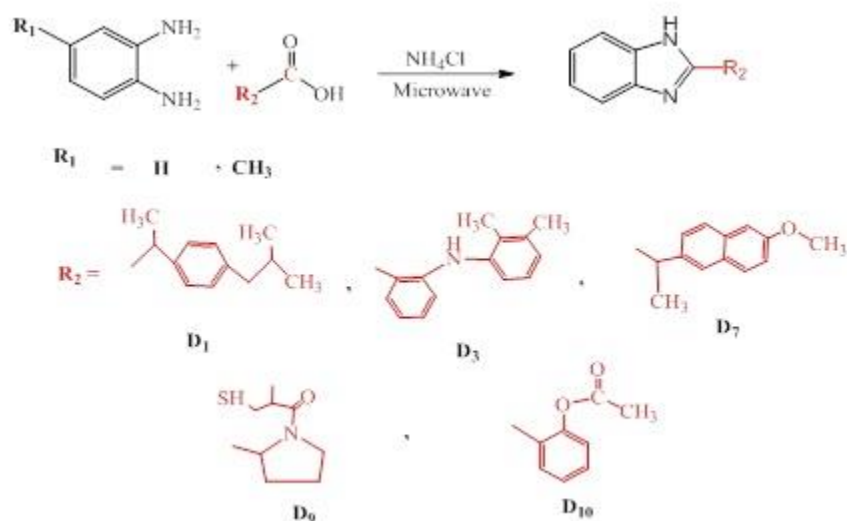


Figure (2): Synthesis of benzimidazole derivatives (D<sub>1</sub>, D<sub>3</sub>, D<sub>7</sub>, D<sub>9</sub>, D<sub>10</sub>).

Table (1): Some physical properties of the synthesized compounds (D<sub>1</sub>, D<sub>3</sub>, D<sub>7</sub>, D<sub>9</sub>, D<sub>10</sub>).

Comp. No.	R <sub>1</sub>	Molecular Formula	Molecular Weight	Color	M.P °C	Yield %	R <sub>f</sub>
D <sub>1</sub>	H	C <sub>19</sub> H <sub>22</sub> N <sub>2</sub>	278.40	Gray	158-160	88	0.64

D <sub>3</sub>	H	C <sub>21</sub> H <sub>19</sub> N <sub>3</sub>	313.40	Brown	192-196	93	0.48
D <sub>7</sub>	CH <sub>3</sub>	C <sub>21</sub> H <sub>20</sub> N <sub>2</sub> O	316.40	Brown	116-119	83	0.58
D <sub>9</sub>	CH <sub>3</sub>	C <sub>16</sub> H <sub>21</sub> N <sub>3</sub>	303.42	Light brown	163-165	94	0.75
D <sub>10</sub>	CH <sub>3</sub>	C <sub>16</sub> H <sub>14</sub> N <sub>2</sub> O <sub>2</sub>	266.30	Brown	196-200	69	0.46

### Synthesis Particles from Graphene Oxide – benzimidazole compound

Apply 0.5 mg of prepared graphene oxide in 10 ml of dioxane and ultrasound for 30 minutes, then add 0.5 mg of one of the prepared benzimidazole compound (D<sub>1</sub>, D<sub>3</sub>, D<sub>7</sub>, D<sub>9</sub>, D<sub>10</sub>,) and heat the mixture for 4 hours at 100 C °. Collect the product and wash with 3 ml deionized water three times and then dried in the oven at 80 C ° [8].

## Results and Discussion

### Discussion of Graphene oxide (GO) nanoparticles

Graphite is the raw material for the preparation of graphene oxide (GO) from polycrystalline molecules or granules that can be from natural or industrial sources. Natural graphite is the most common source. The first step was the preparation of the graphene oxide (GO) (Hummer method) through the interaction of active groups in the caravan structures with oxidation and acid factors for the preparation of the graphene oxide [9]. according mechanism showed in Figure (3)



Figure (3): Mechanism of the prepared of graphene oxide (GO)

The infrared spectrum of nanoparticles of graphene oxide showed a distinctive and broad beam of alcoholic hydroxyl and carboxylic intertwined at 3470 cm<sup>-1</sup> with a broad and strong beam. The measurement also showed two packages at (1230, 1734) cm<sup>-1</sup>. It is another characteristic package which is stretched (νC - O, νC = O). In the carboxyl group respectively, at (1616) cm<sup>-1</sup> attributed to the double stretched stretch (νC = C). The graphene oxide contains epoxy aggregates on the surface of the plate represented by stretched (C - O). These groups were clearly observed at (1230 - 1053) cm<sup>-1</sup> which show a wide beam overlapping with the bending beam. The νOH group is broad and partially overlapping with the bending beam at (1431) cm<sup>-1</sup>. Two beams indicate the presence of aliphatic groups (such as CH<sub>2</sub>), which are produced by tomatoes, which give some acyl terminal groups. And supported by (CH) apparently pure at

(2818 - 2823)  $\text{cm}^{-1}$  [10]. The concentration is very low as evident by the intensity of absorption. Figure (4) shows the infrared spectrum (FT-IR) of graphene oxide

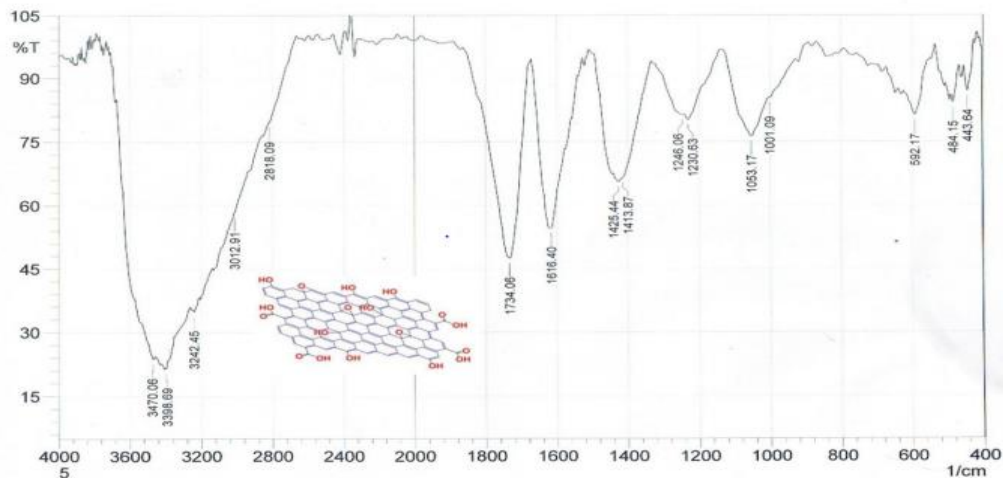
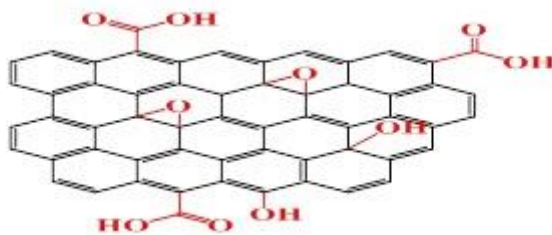


Figure (4): Infrared spectrum (FT - IR) of the compound (GO)

The X-Ray Diffraction (XRD) of graphene oxide shows a large interlayer spacing equal to  $7.745 \text{ \AA}$  at the position  $2\theta = 11.4244^\circ$  with  $\text{FWHM} = 0.5904^\circ$  [11-15]. The disappearance of the peak at approximately  $27^\circ$  due to completely oxidized and ex-exfoliation of graphite after the chemical oxidation Scheme (1). The Figure (5) below shows the XRD of graphene oxide. The widening of the interlayer is solid evidence for the success of the reaction as it is equal no more than  $3.35 \text{ \AA}$  in the graphite [11].



Scheme (1): Graphene oxide (GO) structure.

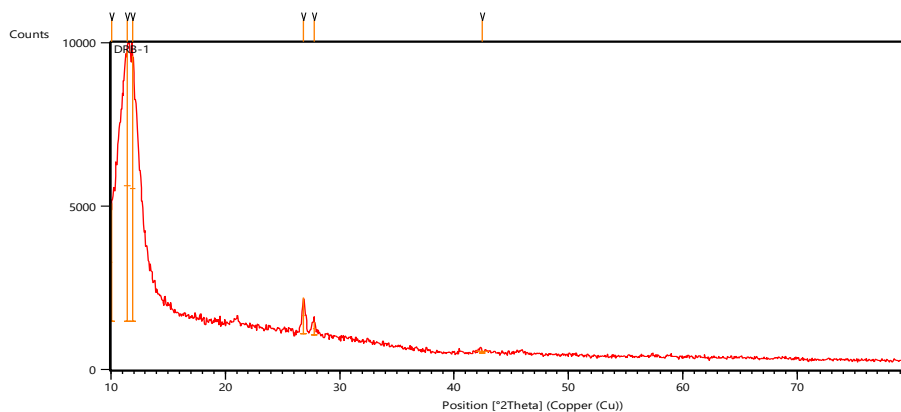


Figure (5): The X-ray diffraction spectrum (XRD) of the compound (GO)

## Diagnosis of benzimidazole compound

The benzimidazole derivatives were synthesized by condensation of O-Phenylenediamine and 4-methyl-O-Phenylenediamine with different carboxylic acids using ammonium chloride as ring closing.

The IR spectrum of compounds (D<sub>1</sub>, D<sub>3</sub>, D<sub>7</sub>, D<sub>9</sub>, D<sub>10</sub>) showed the absence of a  $\nu(2\text{NH}_2)$  band and that presence of a band at (3251-3222  $\text{cm}^{-1}$ ) assign to  $\nu(\text{N-H})$ , also showed band within (1614-1652  $\text{cm}^{-1}$ ) assign to  $\nu(\text{C=N})$ , also showed bands within (3014-3080  $\text{cm}^{-1}$ ) assign to  $\nu(\text{C-H})$  aromatic, also showed two bands (2914-2985  $\text{cm}^{-1}$ ) and (2840-2952  $\text{cm}^{-1}$ ) assign to  $\nu(\text{C-H})$  aliphatic, also showed two bands (1535- 1579  $\text{cm}^{-1}$ ) and (1493-1562  $\text{cm}^{-1}$ ) assign to  $\nu(\text{C=C})$  aromatic. The showed of other bands within (1231-1294  $\text{cm}^{-1}$ ) assign to  $\nu(\text{C-N})$ , The rest of the bands maintained their normal ranges, as shown in Table 2, which shows the results of infrared absorption of synthesis compounds (D<sub>1</sub>, D<sub>3</sub>, D<sub>7</sub>, D<sub>9</sub>, D<sub>10</sub>) [16].

Table (2): FT-IR spectral data for compounds (D<sub>1</sub>-D<sub>5</sub>)

Comp. No.	IR (KBr) $\text{cm}^{-1}$						Others
	$\nu(\text{N-H})$ Benzimida Zole	$\nu(\text{C-H})$ Arom.	$\nu(\text{C-H})$ Aliph.	$\nu(\text{C=N})$	$\nu(\text{C=C})$ Arom.	$\nu$ (C-N)	
D <sub>1</sub>	3242	3014	2960 2923	1623	1579 1514	1294	-----
D <sub>3</sub>	3238	3074	2914 2856	1652	1571 1500	1253	$\nu(\text{N-H})$ 3323
D <sub>7</sub>	3222	3016	2916 2840	1638	1573 1562	1255	$\nu(\text{C-O})$ 1184
D <sub>9</sub>	3251	3076	2955 2842	1626	1535 1493	1231	$\nu(\text{S-H})$ 2569
D <sub>10</sub>	3226	3080	2985 2952	1614	1571 1502	1245	$\nu(\text{C=O})$ 1714

The proton nuclear magnetic resonance spectrum ( $^1\text{H-NMR}$ ) of the synthesis benzimidazole compound (D<sub>3</sub>) it showed a single signal at the site ( $\delta$  2.08, 2.27 ppm) assign to Protons two groups ( $\text{CH}_3$ ) connected to benzene ring, Also a single signal showed at ( $\delta$  2.49 ppm) assign to Solvent (DMSO), Also a single signal showed at ( $\delta$  3.43 ppm) assign to Protons ( $\text{H}_2\text{O}$ ), Multiple signal is showed at the site ( $\delta$  6.66-7.88 ppm) assign to the aromatic ring protons, Also a single signal showed at ( $\delta$  9.45 ppm) assign to Protons group (NH) connected with the two benzene ring, Also a single signal showed at ( $\delta$  12.04 ppm) assign to Protons group (NH) for the imidazole ring [16,17]. As shown in Figure (6).

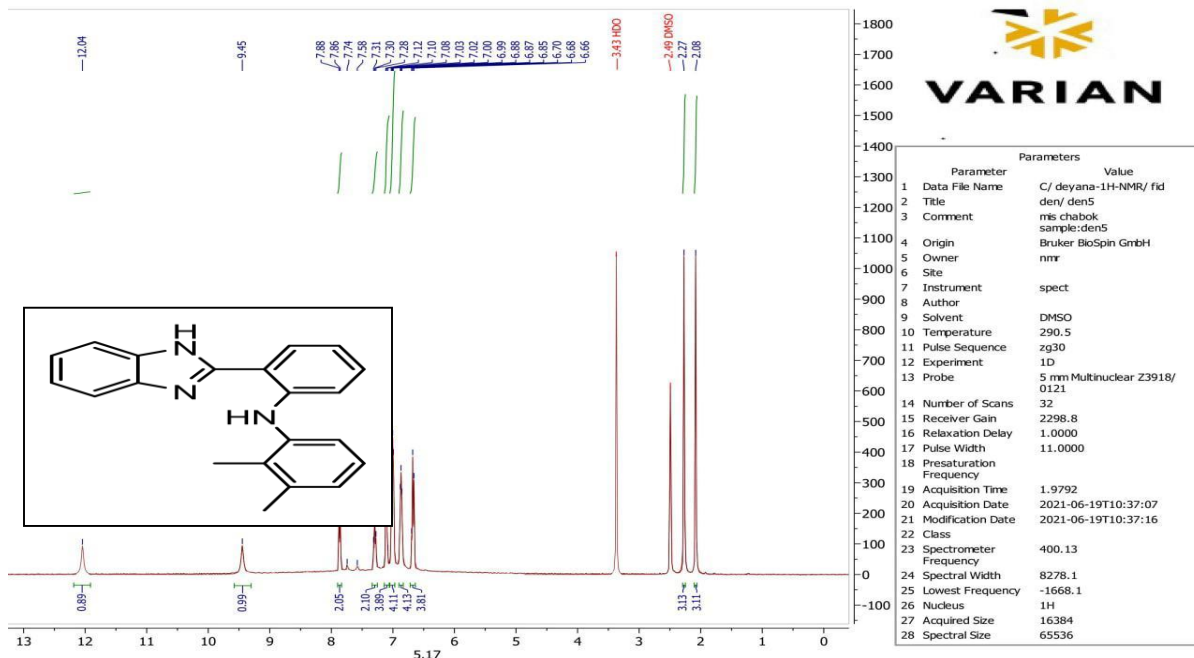


Figure (6): The ( $H^1$ -NMR) of the compound ( $D_3$ )

And studying the  $H^1$ -NMR spectrum of the synthesis benzimidazole compound ( $D_{10}$ ) it showed a single signal showed at ( $\delta$  2.07ppm) assign to Protons group ( $CH_3$ ) for the imidazole ring, Also a single signal at the site ( $\delta$  2.67ppm) assign to Protons groups ( $CH_3$ ) connected to benzene ring, Also a single signal showed at ( $\delta$  2.49 ppm) assign to Solvent (DMSO- $d_6$ ), Also a single signal showed at ( $\delta$  3.63 ppm) assign to Protons ( $H_2O$ ), Multiple signal is showed at the site ( $\delta$  6.90-7.79 ppm) assign to the aromatic ring protons, Also a single signal showed at ( $\delta$  11.27ppm) assign to Protons group (NH) for the imidazole ring. As shown in Figure (7).

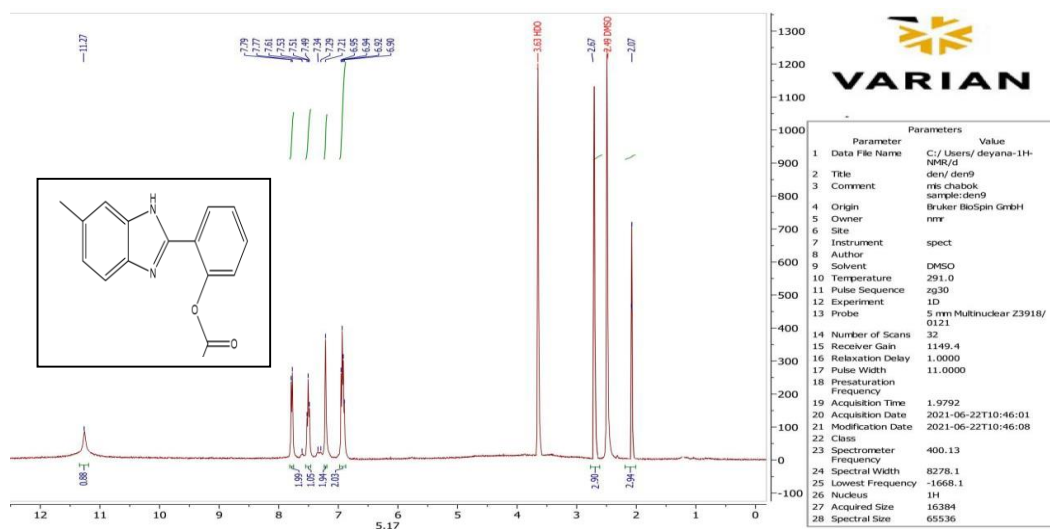


Figure (7): The ( $H^1$ -NMR) of the compound ( $D_{10}$ )

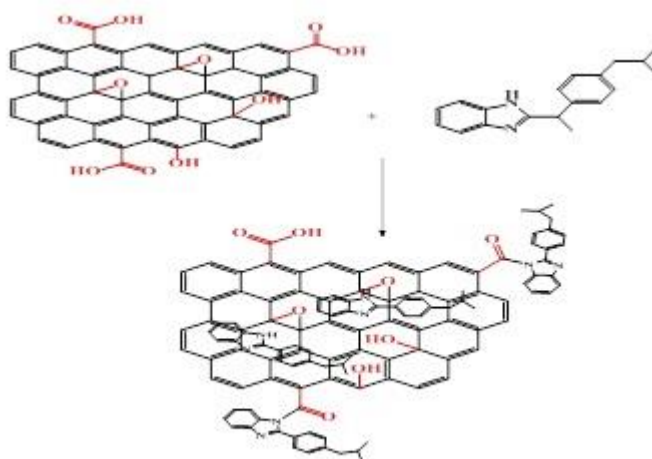
## Diagnosis of particle from graphene Oxide - benzimidazole compound

The nanoparticles were prepared by the graphene oxide dissolved in distilled water with of benzimidazole compound (D<sub>1</sub>, D<sub>3</sub>, D<sub>7</sub>, D<sub>9</sub>, D<sub>10</sub>) and heated for 4 hours to provide aromatic rings on the surface of the plates [18]. The synthesized preparations were diagnosed with fixation of some of their physical The (FT-IR) spectrum of nano Composites (DM<sub>1</sub>, DM<sub>3</sub>, DM<sub>7</sub>, DM<sub>9</sub>, DM<sub>10</sub>) showed the absence of  $\nu(\text{N-H})$ , and absence of  $\nu(\text{O-H})$ .

### GO-2-(4-isobutylphenyl)-1H-benzo[d]imidazole:( DM<sub>1</sub>)

#### XRD analysis of GO-2-(4-isobutylphenyl)-1H-benzo[d]imidazole:

The X-Ray diffraction (XRD) of GO-2-(4-isobutylphenyl)-1H-benzo[d]imidazole shows a medium intense peak at the position ( $2\theta = 10.2644^\circ$ ) due to the remaining of some carboxyl groups out of the chemical bonding (incomplete functionalizing of GO with the added amine), furthermore it refers to the presence of physical adsorption of "2-(4-isobutylphenyl)-1H-benzo[d]imidazole" molecules on the surface of GO, as shown in Scheme (2) [19]. The XRD also shows main peaks at  $2\theta = 12.0534, 16.864, 19.8358, 22.3331, 24.4679, 26.5916,$  and  $35.1224$  which refers to the reflection by crystal planes with miller indices as 111, 200, 220, 311, 321, 410, 420 and 530, respectively, the Figure (8) below shows the XRD pattern of GO-(4-isobutylphenyl)-1H-benzo[d]imidazole compound. Lastly, the results prove the occurrence of two types of bonding, which is the chemical (with the highest percentage) through the formation of amide bonds and the physical bond (with the lowest percentage). The lower and higher ratio was determined based on the intensity of the graphene oxide peak, which was observed to have a significantly lower intensity compared to the graphene oxide alone.



Scheme (2) Synthesis of GO-(4-isobutylphenyl)-1H-benzo[d]imidazole(DM<sub>1</sub>)

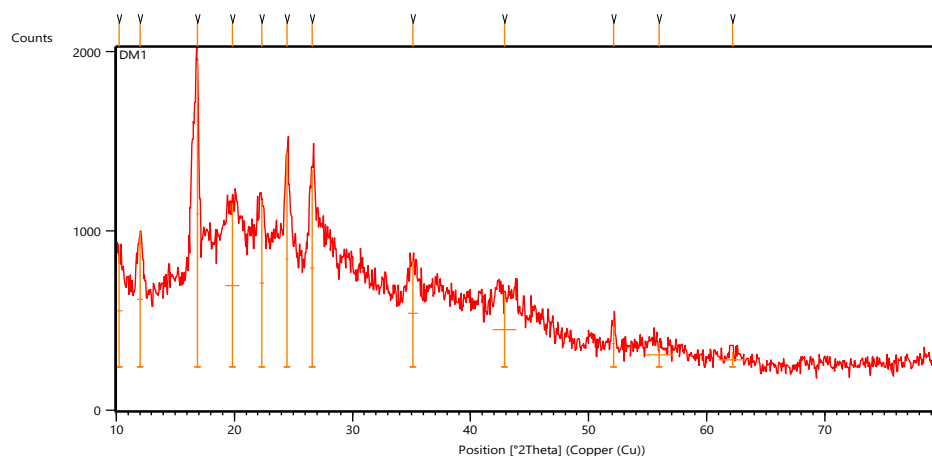


Figure (8): XRD pattern of GO-(4-isobutylphenyl)-1H-benzo[d]imidazole(DM<sub>1</sub>)

### SEM image of GO-2-(4-isobutylphenyl)-1H-benzo[d]imidazole

The scanning electron microscope (SEM) of GO-2-(4-isobutylphenyl)-1H-benzo[d]imidazole showed irregular nano-sheets structures of varying shapes and sizes, with sheet thicknesses ranging from 11.3-53.7 nm. The SEM also revealed large interspaces between nanosheets (porosity) up to 150 nm, which indicates of the high porosity of this sample. As shown in Figure (9).

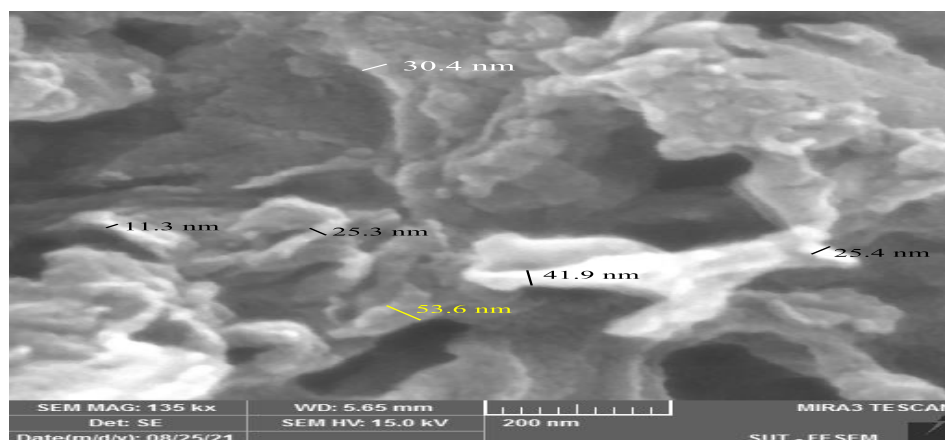


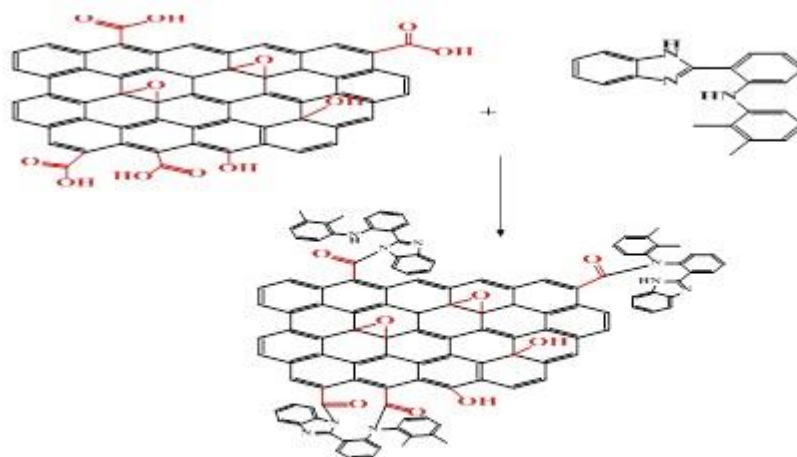
Figure (9): SEM image of GO-2-(4-isobutylphenyl)-1H-benzo[d]imidazole (DM<sub>1</sub>)

### GO- N-(2-(1H-benzo[d]imidazol-2-yl) phenyl)-2,3-dimethylaniline(DM<sub>3</sub>)

#### XRD analysis of GO- N-(2-(1H-benzo[d]imidazol-2-yl) phenyl)-2,3-dimethylaniline:

The completely disappearing of the peak at the position ( $2\theta = 11.4244^\circ$ ) of GO is solid evidence for the chemical functionalizing "[20]" of N-(2-(1H-benzo[d]imidazol-2-yl) phenyl)-2,3-dimethylaniline to the GO to afford GO- N-(2-(1H-benzo[d]imidazol-2-yl) phenyl)-2,3-dimethylaniline as shown in Scheme (3). The peaks at 13.6977, 14.9667, 16.8000, 20.1397, 21.3124, 25.2622, 26.2839 and 27.8090 due to the planes 210, 211, 220, 311, 320, 411, 331 and 332, respectively as shown in the Figure (9). However, there are three possible reaction ways as shown in the Figure 3: reaction of endocyclic NH, exocyclic NH and/ or both of them with OH of

carboxylic acid. This can be attributed to the fact that selectivity cannot be achieved with the presence of the large number of carboxyl groups.



Scheme (3) Synthesis of GO- N-(2-(1H-benzo[d]imidazol-2-yl) phenyl)-2,3-dimethylaniline(DM<sub>3</sub>)

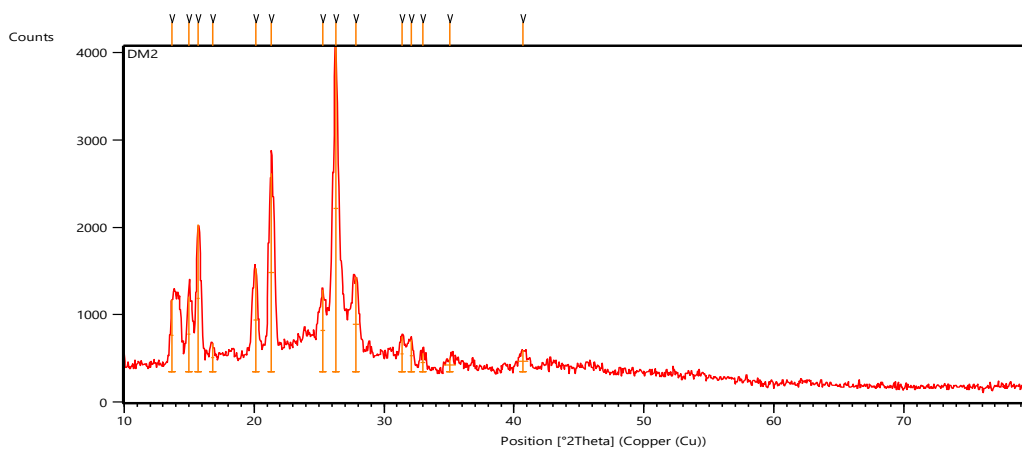


Figure (9) XRD pattern of GO- N-(2-(1H-benzo[d]imidazol-2-yl) phenyl)-2,3-dimethylaniline(DM<sub>3</sub>)

### SEM image of GO- N-(2-(1H-benzo[d]imidazol-2-yl) phenyl)-2,3-dimethylaniline

The scanning electron microscope (SEM) of GO- N-(2-(1H-benzo[d]imidazol-2-yl) phenyl)-2,3-dimethylaniline showed irregular nano-folds which also with varying shapes and sizes, and the particle diameters ranging 19.8-60.6 nm. The SEM also revealed interspaces between nanoparticles up to 123 nm, which indicates that the sample has good porosity, as shown in Figure (10).

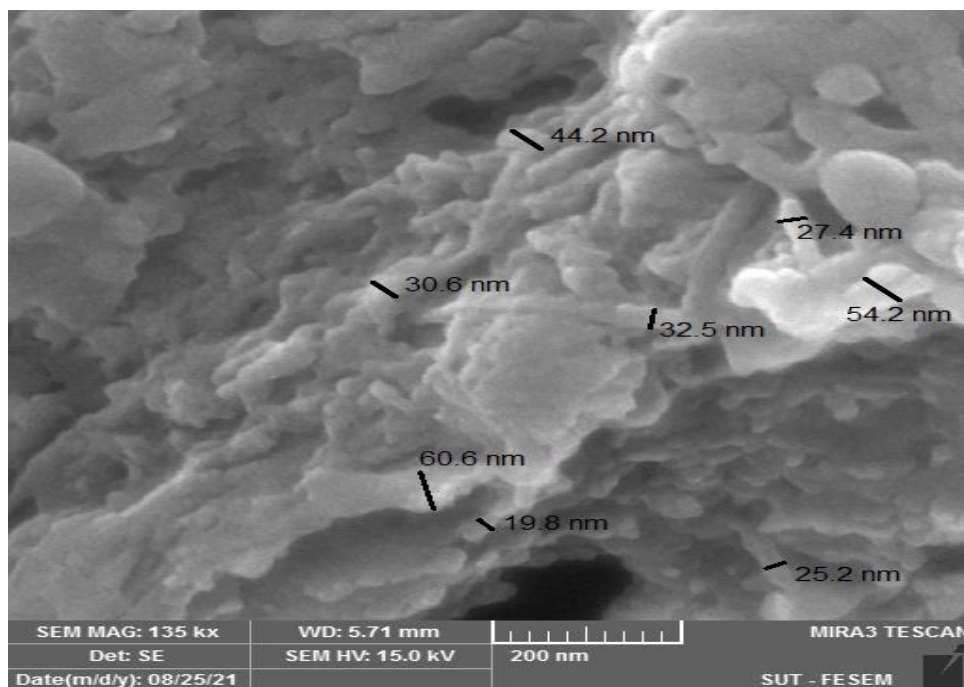


Figure (10): SEM image of GO- N-(2-(1H-benzo[d]imidazol-2-yl) phenyl)-2,3-dimethylaniline(DM<sub>3</sub>)

**AFM for GO-2-(4-isobutylphenyl)-1H-benzo[d]imidazole**

Atomic force microscope (AFM) of GO-2-(4-isobutylphenyl)-1H-benzo[d]imidazole shows a difference from the SEM image as it shows a flat sheet-like nanostructure with a valley. Additionally, the AFM shows nanoparticles with a maximum height of 25.57 nm and diameters ranging between 38.4-197.8 nm. This topography appears clearly in the three-dimensional image (Fig 11-a), while the valley appears in the form of a black opaque area and the nanoparticles with white dots in the two-dimensional imaging (Fig 11-b). Whilst, the AFM measurement showed that the total roughness (which represents the difference in height between the valley and peaks) is equal to 71.41 nm and the Diagram (1) shows the particle size distribution (nm) for this sample.

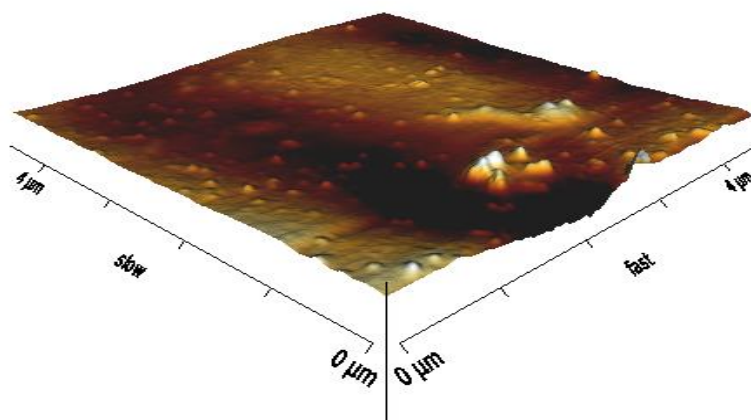


Figure (11-a) AFM 3D image for GO-2-(4-isobutylphenyl)-1H-benzo[d]imidazole(DM<sub>3</sub>)

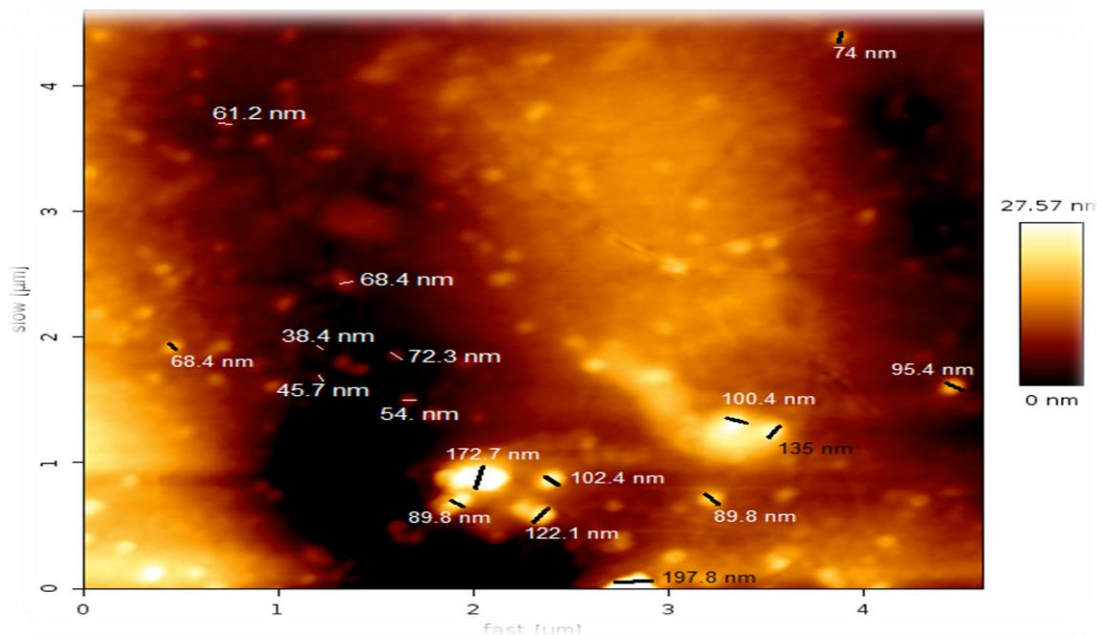


Figure (11-b) AFM 2D image for GO-2-(4-isobutylphenyl)-1H-benzo[d]imidazole(DM<sub>3</sub>)

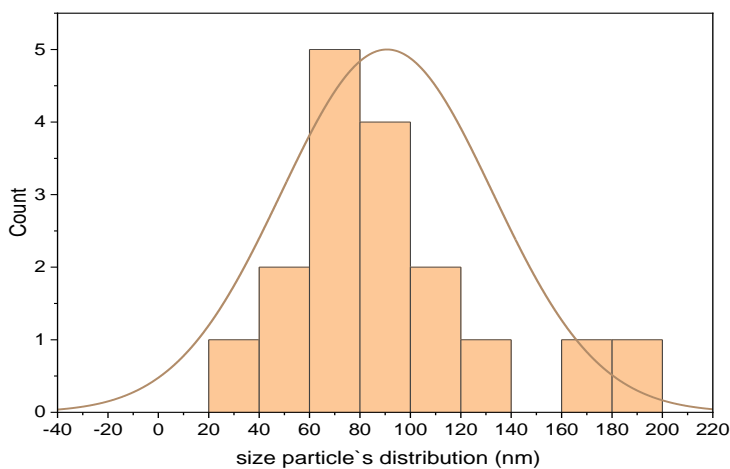


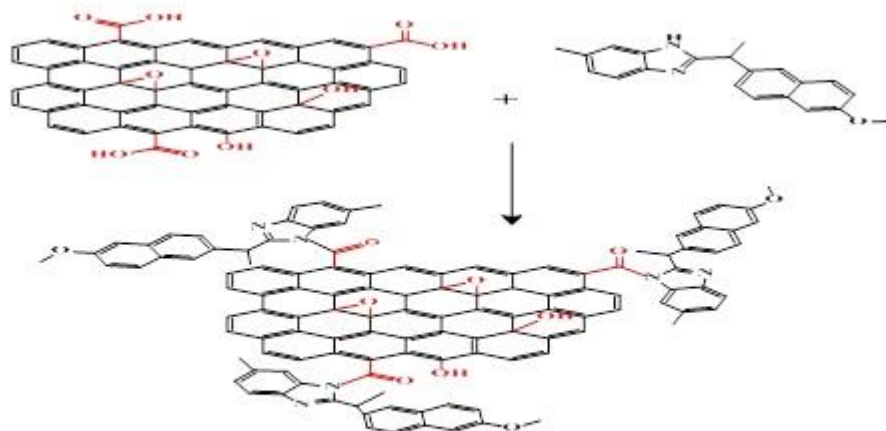
Diagram (1) Particle size distribution (nm) for GO-2-(4-isobutylphenyl)-1H-benzo[d]imidazole (DM<sub>3</sub>)

### GO-2-((6-methoxynaphthalen-2-yl) methyl)-6-methyl-2,7a-dihydro-1H-benzo[d]imidazole(DM<sub>7</sub>)

#### XRD analysis of GO-2-((6-methoxynaphthalen-2-yl) methyl)-6-methyl-2,7a-dihydro-1H-benzo[d]imidazole

Disappearing of the peak at the position ( $2\theta = 11.4244^\circ$ ) of GO proves that the chemical functionalization through formation a new chemical bonding of all carboxyl groups with 2-((6-methoxynaphthalen-2-yl)methyl)-6-methyl-2,7a-dihydro-1H-benzo[d]imidazole to afford GO-GO-2-((6-methoxynaphthalen-2-yl)methyl)-6-methyl-2,7a-dihydro-1H-benzo[d]imidazole as

shown in Scheme (4) The peaks at  $2\theta = 17.9079$ ,  $22.1099$ ,  $27.9451$ ,  $35.3149$  and  $46.1746$  refer to 111, 300, 320, 420, 440 and 710 miller indices respectively as shown in the Figure (12).



Scheme (4) Synthesis of GO-2-((6-methoxynaphthalen-2-yl) methyl)-6-methyl-2,7a-dihydro-1H-benzo[d]imidazole (DM<sub>7</sub>)

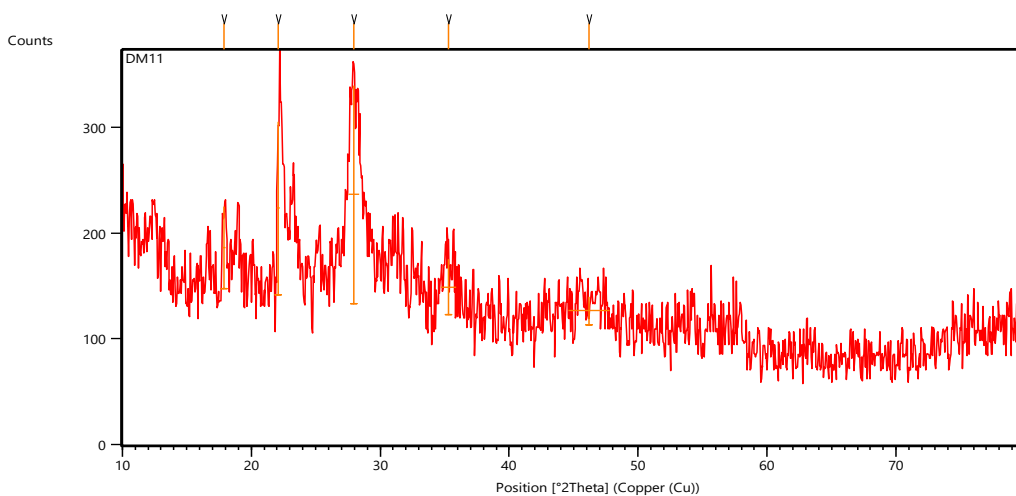


Figure (12): XRD pattern of GO-2-((6-methoxynaphthalen-2-yl) methyl)-6-methyl-2,7a-dihydro-1H-benzo[d]imidazole (DM<sub>7</sub>)

### SEM image of GO-2-((6-methoxynaphthalen-2-yl) methyl)-6-methyl-2,7a-dihydro-1H-benzo[d]imidazole

The scanning electron microscope (SEM) of GO-2-((6-methoxynaphthalen-2-yl) methyl)-6-methyl-2,7a-dihydro-1H-benzo[d]imidazole showed irregular folded nano-sheets. The edges diameters of these folded sheets ranged between 16.3-85.2 nm. Moreover, very few interspaces revealed between nanoparticles were up to 99 nm, which indicates that the sample has few porosity, as shown in Figure (13).

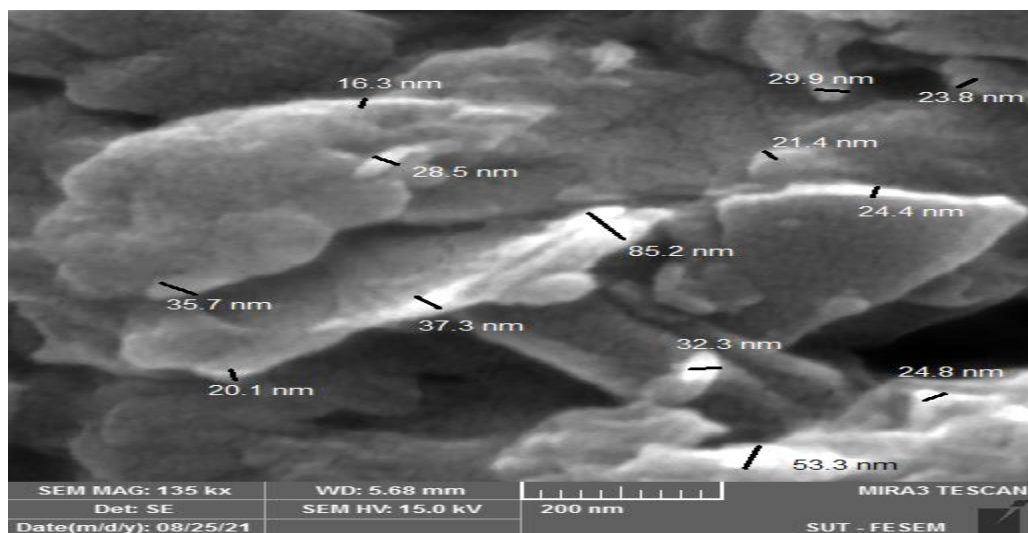
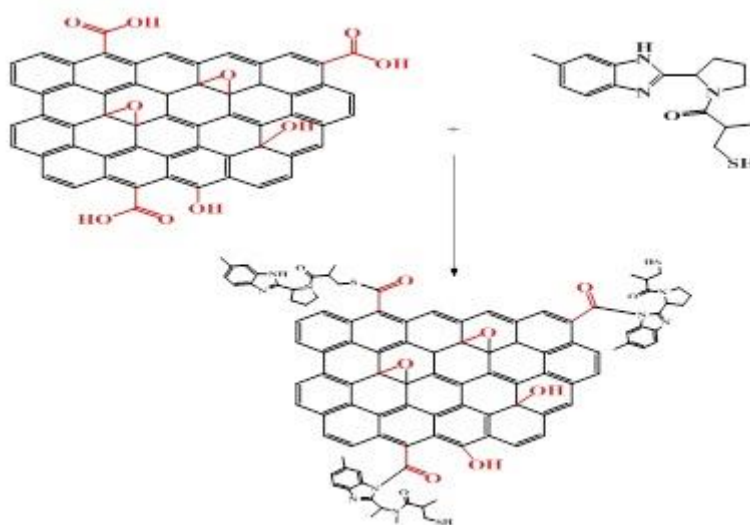


Figure (13) SEM image of GO-2-((6-methoxynaphthalen-2-yl) methyl)-6-methyl-2,7a-dihydro-1H-benzo[d]imidazole (DM<sub>7</sub>)

**GO- 3-mercapto-2-methyl-1-(2-(6-methyl-1H-benzo[d]imidazol-2-yl) pyrrolidin-1-yl) propan-1-one(DM<sub>9</sub>)**

**XRD analysis of GO- 3-mercapto-2-methyl-1-(2-(6-methyl-1H-benzo[d]imidazol-2-yl) pyrrolidin-1-yl) propan-1-one**

The completely disappearing of the peak at the position ( $2\theta = 11.4244^\circ$ ) of GO is solid evidence for the chemical functionalizing of 3-mercapto-2-methyl-1-(2-(6-methyl-1H-benzo[d]imidazol-2-yl) pyrrolidin-1-yl) propan-1-one to the GO to afford GO- 3-mercapto-2-methyl-1-(2-(6-methyl-1H-benzo[d]imidazol-2-yl) pyrrolidin-1-yl) propan-1-one as shown in Scheme (5). The XRD also give new diffraction peaks at  $2\theta = 16.4613, 19.179, 20.3233, 23.4645, 24.0806, 26.095, 27.6728$  and  $29.4462$  which refer to 211, 220, 300, 222, 320, 321, 410 and 331 miller indices, respectively. As shown in the Figure (14), there are two suggested reactions via the endocyclic nitrogen atom of NH group or the terminal sulfur atom of SH group.



Scheme (5) preparing of GO- 3-mercapto-2-methyl-1-(2-(6-methyl-1H-benzo[d]imidazol-2-yl) pyrrolidin-1-yl) propan-1-one (DM<sub>9</sub>)

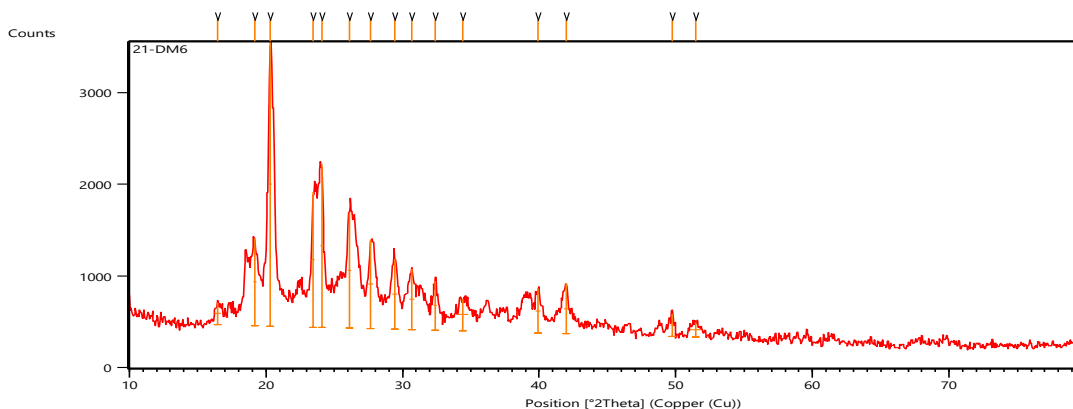


Figure (14): XRD pattern of GO- 3-mercapto-2-methyl-1-(2-(6-methyl-1H-benzo[d]imidazol-2-yl) pyrrolidin-1-yl) propan-1-one (DM<sub>9</sub>)

**SEM image of GO- 3-mercapto-2-methyl-1-(2-(6-methyl-1H-benzo[d]imidazol-2-yl) pyrrolidin-1-yl) propan-1-one**

The scanning electron microscope of GO- 3-mercapto-2-methyl-1-(2-(6-methyl-1H-benzo[d]imidazol-2-yl) pyrrolidin-1-yl) propan-1-one showed irregular layers with varying shapes and sizes. The diameters of the top of layers ranged between 23.9-64.9 nm. On the other hand, interspaces were revealed between nanoparticles up to 65.6 nm, which indicates that the sample has some porosity, as shown in Figure (15).

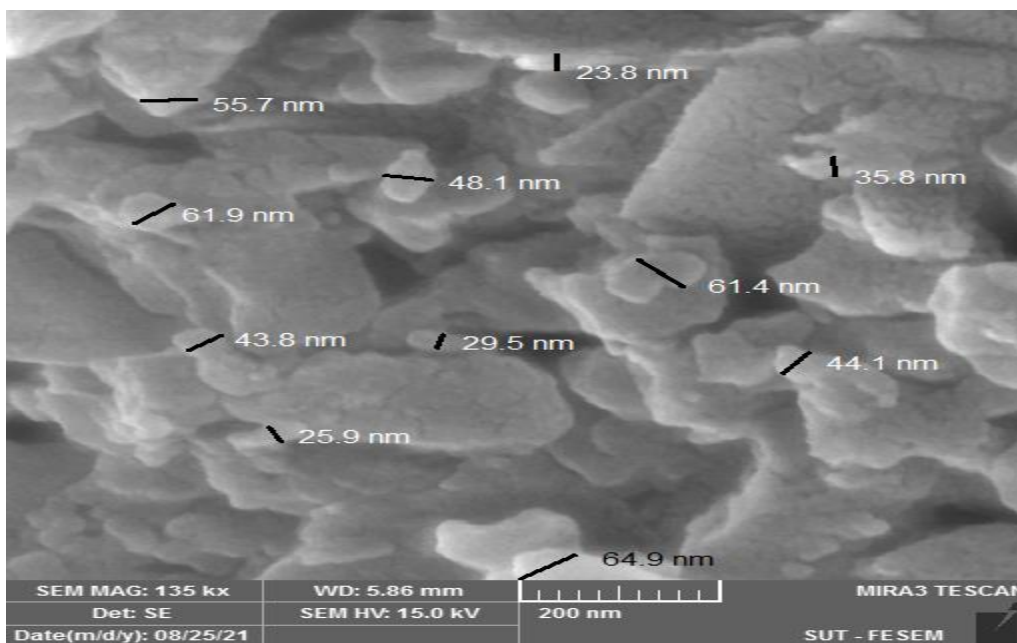


Figure (15): SEM image of GO- 3-mercapto-2-methyl-1-(2-(6-methyl-1H-benzo[d]imidazol-2-yl)pyrrolidin-1-yl)propan-1-one(DM<sub>9</sub>)

## AFM for GO- 3-mercapto-2-methyl-1-(2-(6-methyl-1H-benzo[d]imidazol-2-yl) pyrrolidin-1-yl) propan-1-one

Atomic force microscope of GO- 3-mercapto-2-methyl-1-(2-(6-methyl-1H-benzo[d]imidazol-2-yl) pyrrolidin-1-yl) propan-1-one sample shows nanostructures that similar to the GO- 1,2-bis(1H-benzo[d]imidazol-2-yl) ethane-1,2-diol sample but with fewer nanoparticles and lower heights with maximum height 6.581 nm, thus in the 3D AMF image, these nanoparticles were clearly appeared with existing of some grooves Fig (16-a) which appeared as dark area, black and bold lines in 2D AMF image Fig (16-b). Finally, the total roughness was 19.19 nm and the particle size distribution (nm) for this sample is shown in Diagram (2).

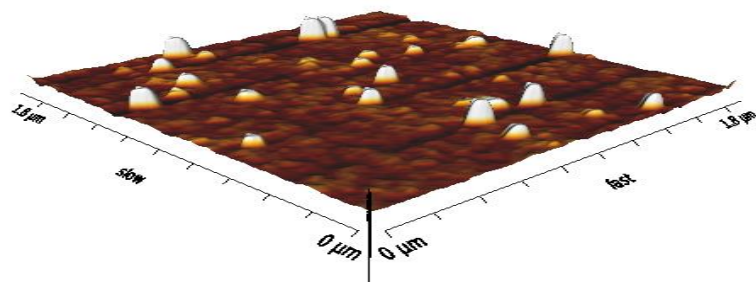


Figure (16-a) AFM 3D image for GO- 3-mercapto-2-methyl-1-(2-(6-methyl-1H-benzo[d]imidazol-2-yl) pyrrolidin-1-yl) propan-1-one

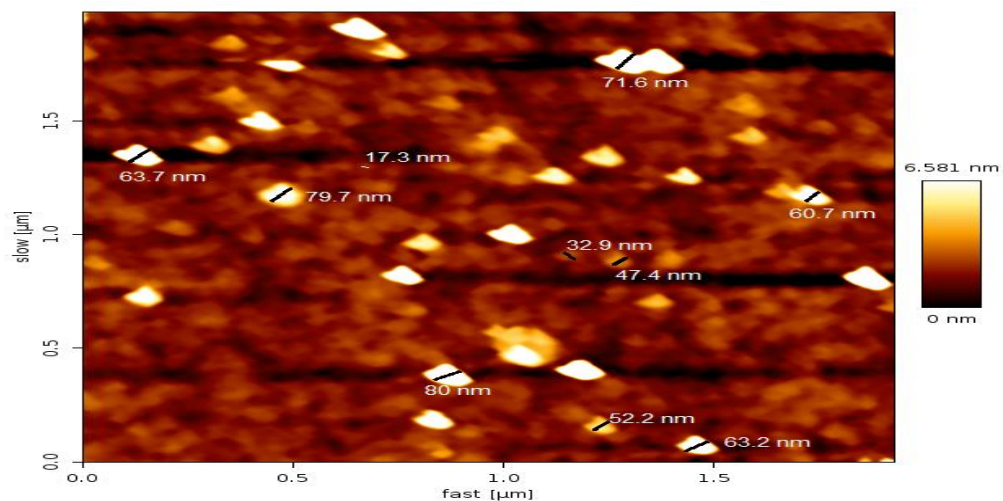


Figure (16-b) AFM 2D image for GO- 3-mercapto-2-methyl-1-(2-(6-methyl-1H-benzo[d]imidazol-2-yl) pyrrolidin-1-yl) propan-1-one

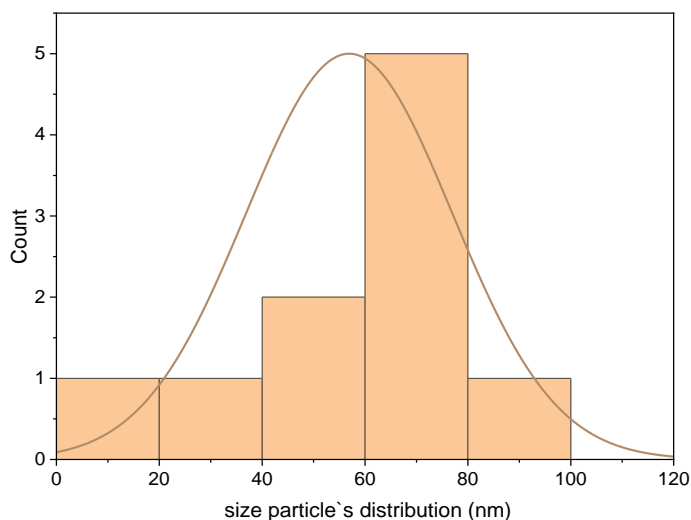
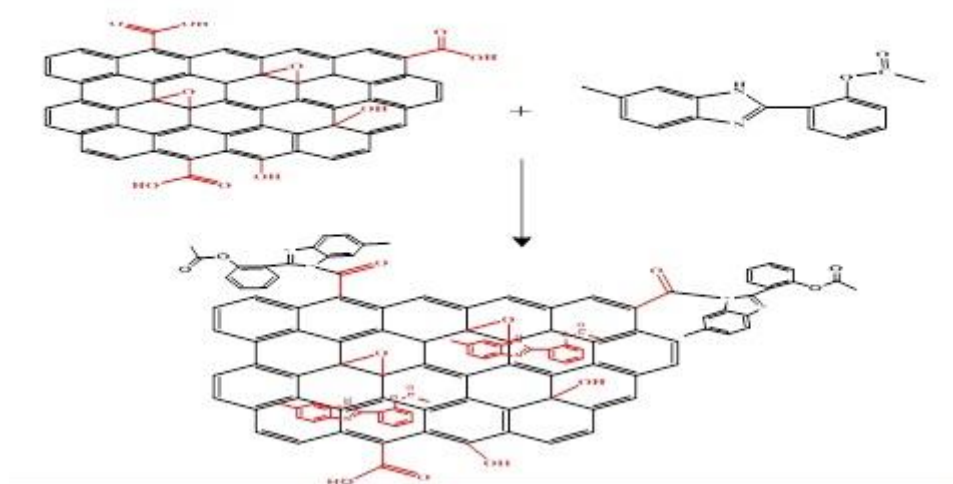


Diagram (2) Particle size distribution (nm) for GO- 3-mercapto-2-methyl-1-(2-(6-methyl-1H-benzo[d]imidazol-2-yl) pyrrolidin-1-yl) propan-1-one.

### **GO-2-(6-methyl-1H-benzo[d]imidazol-2-yl) phenyl acetate(DM<sub>10</sub>)**

#### **XRD analysis of GO-2-(6-methyl-1H-benzo[d]imidazol-2-yl) phenyl acetate**

The X-Ray Diffraction pattern of GO-2-(6-methyl-1H-benzo[d]imidazol-2-yl) phenyl acetate shows a weak peak at position ( $2\theta = 11.5608$ ) which refers to the remaining of some carboxyl groups Which deduce that the functionalization is not chemical functionalization only otherwise there is a physical interaction between GO and 2-(6-methyl-1H-benzo[d]imidazol-2-yl)phenyl acetate during the formation of GO-2-(6-methyl-1H-benzo[d]imidazol-2-yl)phenyl acetate as shown in Scheme (6). The peaks at  $2\theta = 11.5608, 19.4572, 20.8347, 24.0254, 26.5676, 35.0234$  and  $39.751$  due to 111, 220, 310, 321, 400, 511 and 530 miller indices respectively as shown in the Figure (17). These new peaks are a good evidence for the formation of the suggested compound.



Scheme (6) preparing of GO-2-(6-methyl-1H-benzo[d]imidazol-2-yl) phenyl acetate (DM<sub>10</sub>)

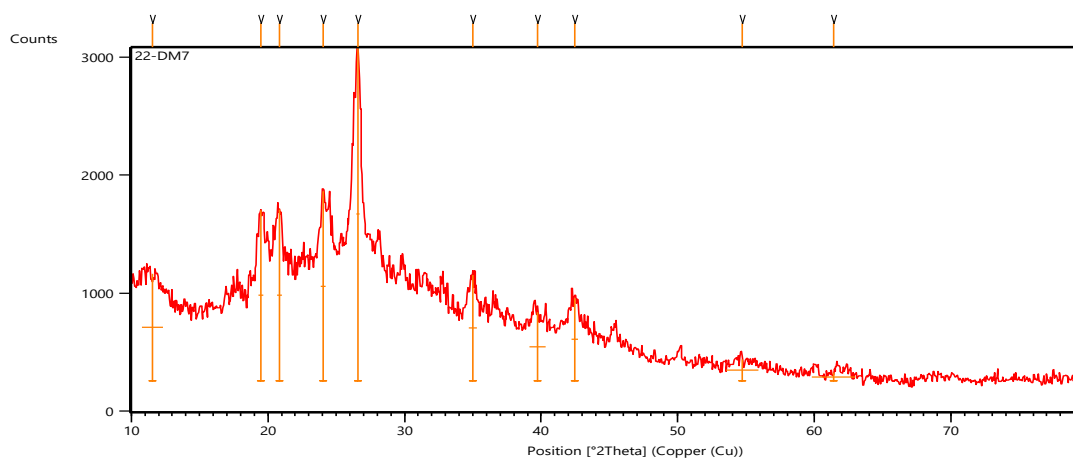


Figure (17) XRD pattern of GO-2-(6-methyl-1H-benzo[d]imidazol-2-yl) phenyl acetate(DM<sub>10</sub>)

### SEM image of GO-2-(6-methyl-1H-benzo[d]imidazol-2-yl) phenyl acetate

The scanning electron microscope of GO-2-(6-methyl-1H-benzo[d]imidazol-2-yl) phenyl acetate showed irregular cracked nanosheets and the diameters of the top of these layers ranged between 17.1-60.7 nm. Besides, few interspaces were revealed between nanoparticles up to 142.6 nm, indicating the sample also has some porosity, as shown in Fig (18).

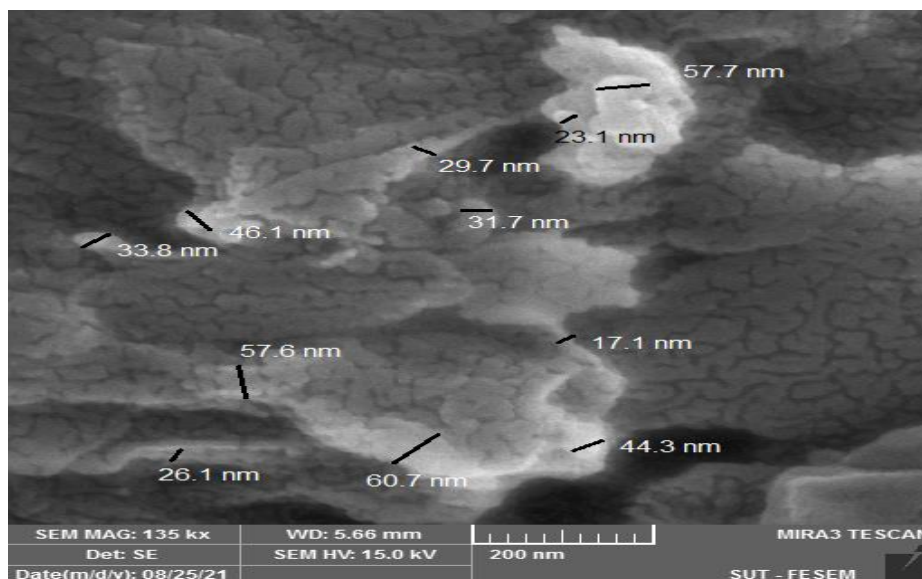


Figure (18): SEM image of GO-2-(6-methyl-1H-benzo[d]imidazol-2-yl) phenyl acetate(DM<sub>10</sub>)

### Evaluation of the biological effectiveness of some synthesis compounds

The effect of some of the synthesis compounds was studied on the growth of one type of a fungus of the yeast variety *Candida* was studied and type of bacterial isolates of *Bacillus Puimilus* and the standard fungicide (Nystatin) of the fungus was used. And the standard antibiotic (neomycin sulfate) of bacteria and the results indicate that the synthesized compounds have the ability to inhibit the fungus and bacteria used by using different concentrations of the concentrated compounds (5mg / ml), (7mg / ml), (10mg / ml) compared with the inhibition with the standard antibodies with concentration (10mg / ml). Some synthesized compounds showed good inhibitory activity against bacteria and weak inhibitory activity against fungi [21,22].

### *Candida albicans* Fungus

All synthesized compounds (DM<sub>1</sub>, DM<sub>3</sub>, DM<sub>7</sub>, DM<sub>9</sub>) showed weak activity at synthesized concentrations (5mg/ml), (7mg/ml), (10mg/ml) as in table (3).

Table (3): Antifungal activity of synthesized compounds (DM<sub>1</sub>, DM<sub>3</sub>, DM<sub>7</sub>, DM<sub>9</sub>)

Comp. No.	Standard 10mg/ml	5mg/ml	7mg/ml	10mg/ml
DM <sub>1</sub>	32.5	15.4	15.6	15.7
DM <sub>3</sub>	33.8	15.8	15.3	16
DM <sub>7</sub>	33.5	14.6	14	15.5
DM <sub>9</sub>	33	15.8	15.7	15.8

## Biological activity of Candida

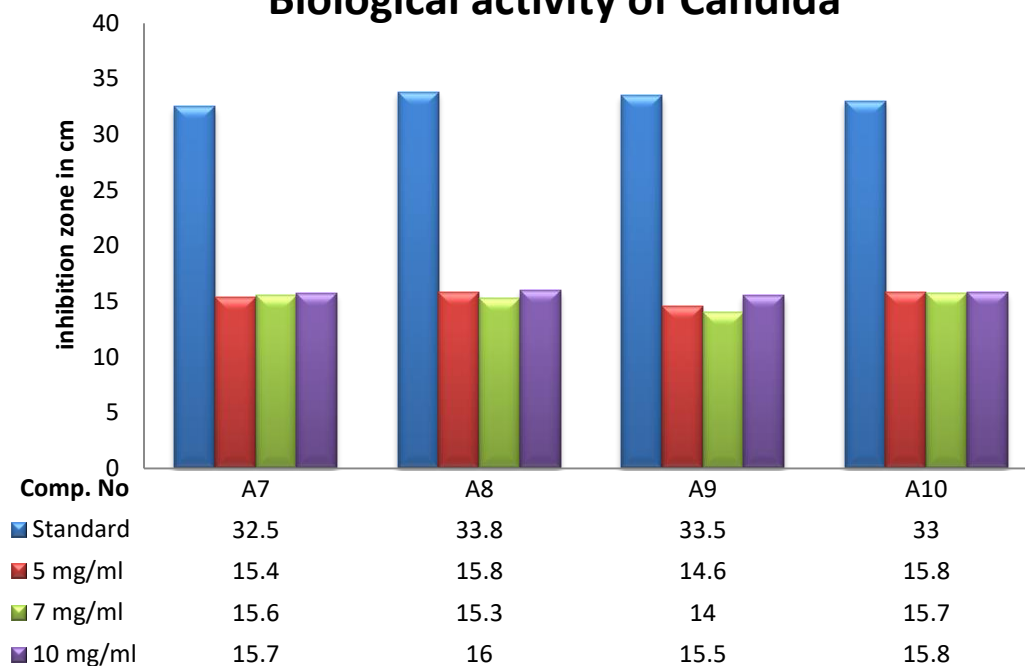


Diagram (3): Inhibitory activity of synthesized compounds (**DM<sub>1</sub>**, **DM<sub>3</sub>**, **DM<sub>7</sub>**, **DM<sub>9</sub>**) against *Candida* fungus

### Bacillus Puimilus

In these bacteria (*Bacillus Puimilus*) all compounds synthesized (**DM<sub>1</sub>**, **DM<sub>3</sub>**, **DM<sub>7</sub>**, **DM<sub>9</sub>**) showed good inhibitory activity at the concentrations (5mg / ml), (7mg / ml) and (10mg / ml) as shown in table (4).

Table (4) antibacterial activity of synthesized compounds (**DM<sub>1</sub>**, **DM<sub>3</sub>**, **DM<sub>7</sub>**, **DM<sub>9</sub>**)

Comp. No.	Standard	5mg/ml	7mg/ml	10mg/ml
<b>DM<sub>1</sub></b>	16.4	15.2	15.4	<b>15.3</b>
<b>DM<sub>3</sub></b>	18	17.1	17.2	<b>17.9</b>
<b>DM<sub>7</sub></b>	16.6	17.2	16.6	<b>16.8</b>
<b>DM<sub>9</sub></b>	17.6	14.1	15.7	<b>15.8</b>

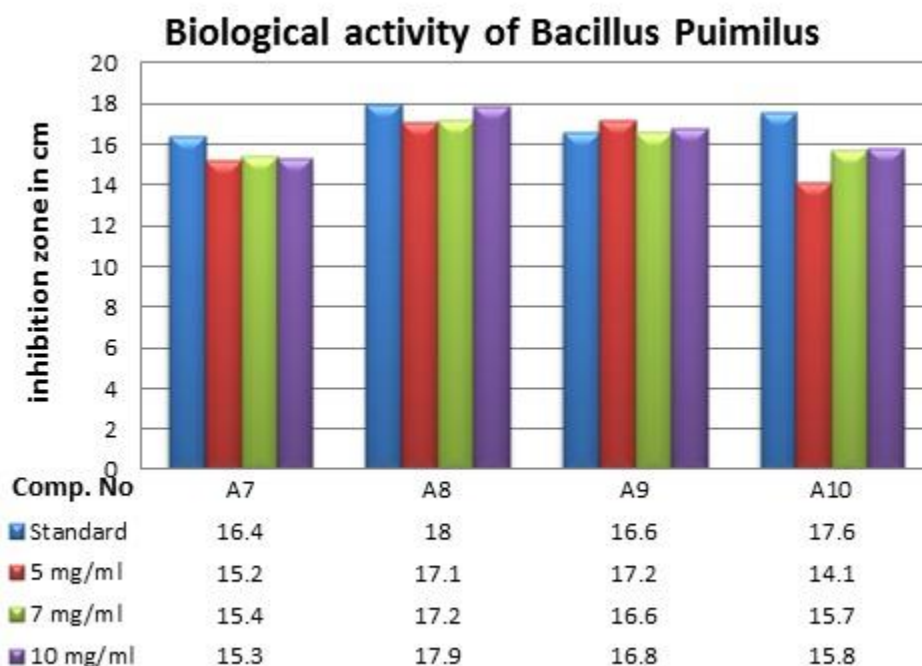


Diagram (4): Inhibitory activity of synthesized compounds (**DM<sub>1</sub>**, **DM<sub>3</sub>**, **DM<sub>7</sub>**, **DM<sub>9</sub>**) against Bacillus Pumilus

## References:

1. Palavicino, C. A., & K, Konrad. (2018). The Rise of Graphene Expectations: Anticipatory Practices in Emergent Nanotechnologies. *Futures*.
2. Geim, A. k. & Novoselov, K. S. (2007). The rise of graphene. *Nature Materials*, 6, pp: 183-191.
3. S, Stankovich., D, A. Piner., R, D. Kohlhaas., K, A. Kleinhammes., & A, Jia. (2007). *Carbon*, 45, 1558.
4. Ajani, O. O., Ezeoke, E. K., Edobor-Osoh, A., & Ajani, O. A. (2013). *Int. Res. J. Pure Applied Chem.*, 3, 10-21.
5. Walia, R., Hedaitullah, Md., Naaz, S. F., Iqbal, K., & Lamba, H. S. (2011). *Int. J. Res. Pharm. Chem.*, 1(3), 565-574.
6. Shahriary, L., & Athawale, A.A. (2014). Graphene oxide synthesized by using modified hummers approach. *Int J Renew Energy Environ Eng*, vol. 2, pp. 58-63.
7. Olyinka, O. Ajani., Damilola V., Aderohunmu., Shade J., Olorunshola, Chinwe. O., Ikpo & Ifedolapo, O. Olanrewaju. (2016). Facile Synthesis, Characterization and Antimicrobial Activity of 2-Alkanamino Benzimidazole Derivatives. *Oriental Journal of Chemistry*. Vol. 32, No. (1): Pg. 109-120
8. L, Issam., T, M. AL-Saad., E, AL-Abodi., & T, A. AL-Dhair. (2011). Seventh Scientific Conference of the Faculty of Education/University of Tikrit Nanotube of Anything Industrial.
9. Tagreed, M. saadi., & Mustafa, A. K. (2016). Preparation of Graphene Flakes and studying Its Structural Properties. *Iraqi Journal of Science*, 57(1): 145-153.
10. A, Ansón-Casaos., J, Puértolas., F, Pascual., J, Hernández-Ferrer., P, Castell., A, M. Benito., & et al. (2014). The effect of gamma-irradiation on few-layered graphene materials. *Applied Surface Science*, vol. 301, pp. 264-272.

11. Abd, A. N., Al-Agha, A. H., Alheety, M. A. (2016). Addition of some primary and secondary amines to graphene oxide, and studying their effect on increasing its electrical properties. *Baghdad Science Journal*, 13(1).
12. Rasheed, M., Shihab, S., & Sabah, O. W. (2021). An investigation of the Structural, Electrical and Optical Properties of Graphene-Oxide Thin Films Using Different Solvents. In *Journal of Physics: Conference Series* (Vol. 1795, No. 1, p. 012052). IOP Publishing.
13. Bashir, B., Khalid, M. U., Aadil, M., Zulfiqar, S., Warsi, M. F., Agboola, P. O., & Shakir, I. (2021).  $Cu_xNi_{1-x}O$  nanostructures and their nanocomposites with reduced graphene oxide: synthesis, characterization, and photocatalytic applications. *Ceramics International*, 47(3), 3603-3613.
14. Nguyen, Q., Rizvandi, R., Karimipour, A., Malekahmadi, O., & Bach, Q. V. (2020). A novel correlation to calculate thermal conductivity of aqueous hybrid graphene oxide/silicon dioxide nanofluid: synthesis, characterizations, preparation, and artificial neural network modeling. *Arabian Journal for Science and Engineering*, 45(11), 9747-9758.
15. Xu, Y., Nguyen, Q., Malekahmadi, O., Hadi, R., Jokar, Z., Mardani, A., Bach, Q. V. (2020). Synthesis and characterization of additive graphene oxide nanoparticles dispersed in water: experimental and theoretical viscosity prediction of non-Newtonian nanofluid. *Mathematical Methods in the Applied Sciences*.
16. Silverstein RM., Webster FX., Kiemle DJ., & Bryce, DL. (2014Sep29). Spectrometric identification of organic compounds. John wiley & sons.
17. Nuclear, T. (2018). Resonance M. Experimental Approaches of NMR Spectroscopy. *Experimental Approaches of NMR Spectroscopy*.
18. C. M. Burba., R. Frech, J. (2006). *Spectrochimica Acta Part A Molecular and Biomolecular Spectroscopy*, 65, 44-50.
19. Georgakilas, V., Tiwari, J. N., Kemp, K. C., Perman, J. A., Bourlinos, A. B., Kim, K. S., & Zboril, R. (2016). Noncovalent functionalization of graphene and graphene oxide for energy materials, biosensing, catalytic, and biomedical applications. *Chemical reviews*, 116(9), 5464-5519.
20. Gao, W. (2015). *The Chemistry of Graphene Oxide*. Springer, Cham., In *Graphene oxide* (pp. 61-95).
21. Rasheed, Malath. K., AL-Rifaie, Diana. A. (2020). Synthesis Some of Thiazolidinone and Tetrazole Compounds Derived From Acriflavine and Evaluation of Their Antimicrobial, Antifungal And Antiox. *Sys Rev Pharm* 11(12).
22. Rasheed, Malath. K., AL-Rifaie, Diana. A., & Madab, Dhameer. (2021). Synthesis and Evaluation of Antibacterial and Antifungal Activity of New 1, 5-Benzodiazepine Derivatives Contain Cyclic Imides and Mannich Bases. *International Journal of Pharmaceutical Research*.

## تحضير وتشخيص بعض مركبات النانو لمشتقات البنزيميدازول ودراسة نشاطها المضاد للبيكتيريا والفطريات

ديانا عبد الكريم الرفاعي<sup>1</sup> ، ملاذ خلف رشيد<sup>2</sup>

قسم الكيمياء ، كلية التربية ، جامعة سامراء ، سامراء ، العراق

### الخلاصة:

في هذه الدراسة، تم تحضير العديد من الجسيمات النانوية لألواح الكرافين، والتي تم تحضيرها باستخدام مركبات البنزيميدازول. تخترق الأوكسدة بين الطبقات داخل بلورات الكرافيت لإزالة الطبقات جزئياً أو كلياً من خلال التقشير الكيميائي، تم تحضير الجسيمات النانوية من الجرافين على خطوتين. كانت الخطوة الأولى هي تحضير أوكسيد الكرافين (طريقة هامر) من خلال تفاعل المجموعات النشطة. في هياكل الكربون مع عوامل الأوكسدة والحامض لتحضير أكسيد الكرافين. كانت الخطوة الثانية هي تصنيع مشتقات بنزيميدازول من تفاعل مركب 4- مثل أورثو فنيلين ثنائي امين وأورثو ينيلين ثنائي امين مع أحماض كربوكسيلية مختلفة في وجود كلوريد الأمونيوم كعامل مساعد، باستخدام طريقة التشعيع بالميكروويف. كانت الخطوة الثالثة هي تفاعل أكسيد الكرافين النانوي مع مشتقات البنزيميدازول. تم استخدام تأثير بعض مركبات النانو على نمو أحد الفطريات لنوع الخميرة المبيضات وعزلات البكتيريا من *Bacillus Puimilus* و *Nystatin* للفطريات وكيريتات النيومايسين للبيكتيريا. وتشير النتائج إلى أن مركبات النانو لديها القدرة على تثبيط الفطريات والبيكتيريا المستخدمة

### معلومات البحث:

تاريخ الاستلام: 2020/00/00

تاريخ القبول: 2020/00/00

الكلمات المفتاحية:

اوكسيد الكرافين البنزيميدازول  
المتراكبات النانوية

معلومات الباحث

## تحضير وتشخيص بعض مركبات النانو لمشتقات البنزيميدازول ودراسة نشاطها المضاد للبكتيريا والفطريات

ديانا عبد الكريم شاكر\*، ملاذ خلف رشيد

قسم الكيمياء، كلية التربية، جامعة سامراء، سامراء، العراق

معلومات البحث:	الخلاصة:
تاريخ الاستلام: 2022/02/04	في هذه الدراسة، تم تحضير العديد من الجسيمات النانوية لألواح الكرافين، والتي تم تحضيرها باستخدام مركبات البنزيميدازول. تخترق الأكسدة بين الطبقات داخل بلورات الكرافيت لإزالة الطبقات جزئياً أو كلياً من خلال التقشير الكيميائي، تم تحضير الجسيمات النانوية من الجرافين على خطوتين. كانت الخطوة الأولى هي تحضير أكسيد الكرافين (طريقة هامر) من خلال تفاعل المجموعات النشطة. في هياكل الكربون مع عوامل الأكسدة والحامض لتحضير أكسيد الكرافين. كانت الخطوة الثانية هي تصنيع مشتقات بنزيميدازول من تفاعل مركب 4- مثل أورثو فنيلين ثنائي امين وأورثو بنيلين ثنائي امين مع أحماض كربوكسيلية مختلفة في وجود كلوريد الأمونيوم كعامل مساعد، باستخدام طريقة التشعيع بالميكروويف. كانت الخطوة الثالثة هي تفاعل أكسيد الكرافين النانوي مع مشتقات البنزيميدازول. تم استخدام تأثير بعض مركبات النانو على نمو أحد الفطريات لنوع الخميرة المبيضات وعزلات البكتيريا من <i>Bacillus Puimilus</i> و <i>Nystatin</i> للفطريات وكبريتات النيومايسين للبكتيريا. وتشير النتائج إلى أن مركبات النانو لديها القدرة على تثبيط الفطريات والبكتيريا المستخدمة
تاريخ القبول: 2022/03/20	
الكلمات المفتاحية:	
أكسيد الكرافين البنزيميدازول المترابكات النانوية	
معلومات المؤلف	
الايمل: 07702646676 الموبايل: 07702646676	